

Research Article

Cooling System Analysis for a Data Center using Liquid Immersed Servers

A. Almanea^{Å*}, H. Thompson^Å, J. Summers^Å and N. Kapur^Å

^ÅInstitute of Engineering Thermofluids (iTF), School of Mechanical Engineering, University of Leeds, LS2 9JT, Leeds, United Kingdom

Accepted 17 Aug 2014, Available online 01 Sept 2014, Vol.4, No.3 (Sept 2014)

Abstract

Data centers are large consumers of power, of which a large proportion is spent on removing the heat generated by the semiconductors inside IT servers. This paper develops a full analysis of the cooling system when servers are immersed in a dielectric liquid and water is used to transport the heat outside of the data center. The analysis combines empirical curve fits and flow analysis with computational fluid dynamics (CFD) simulations of liquid immersed servers placed in parallel in a rack of a data center. The liquid immersed server concept is based on a dielectric liquid that is in direct contact with the semiconductor components to improve heat rejection. The heat generated from the microelectronics is naturally convected, via buoyancy, in the dielectric liquid to a cold plate on the opposing side. The cooling system of the data center in this study consists of a dry air cooler and a liquid-to-liquid buffer heat exchanger. It was found that the power usage effectiveness (PUE) is as low as 1.08 for the cooling system. The results also show that the PUE is affected by the server-rack occupancy and can increase by 26% as occupancy drops by 80%, thus the better the server-rack occupancy, the better the PUE.

Keywords: data center, liquid cooling, power usage effectiveness, liquid immersed servers.

1. Introduction

The increasing demand for digital services today has led to an unprecedented growth globally in data centers and their energy demand. Efficient cooling of data center is needed, since over 30 % of data center power consumption is used for cooling (Greenberg *et al.* 2006; Shah *et al.* 2008). Data centers can be cooled by the more traditional air cooling, but some are now being cooled directly with the aid of liquids (American Society of Heating *et al.* 2006). The latter approach is usually used in data centers with high density racks. The liquid cooling of data centers can be classified in essentially three ways; rack heat exchanger, in server and on chip heat exchangers and total liquid immersion. The heat transfer in the immersed server is by way of natural convection of a dielectric liquid, which transfers the thermal energy produced by the microelectronics into a water jacket, through which a pumped coolant passes (Chester *et al.* 2013; Hopton *et al.* 2013).

The main interest in this paper involves the integration of liquid immersed servers in the whole data center cooling system. The cooling system in this study consists of dry air cooler and buffer heat exchanger, together they can reject the heat from racks via liquid loops. The cooling system is explained in detail in the next sections. The ambient temperature for the calculations in this paper are taken for the city of Leeds (Jensen 2013). A MATLAB program is used to calculate the inlet water temperature to

the rack based on the ambient temperature and pump flow rates. With the evaluated rack inlet flow rate and temperature, a computational model based on COMSOL is used to determine pressure drop for the immersed servers. The power of the pumps can be determined for the pressure drop and flow rate. The power usage effectiveness (PUE) of the data center is calculated from the IT power consumption and power consumed by the pumps and fans in the cooling loop. The variation of PUE is determined with varying rack load and is also presented.

2. Cooling data center system

A schematic diagram of the data centre cooling system that is used in this section is shown in Fig.1.

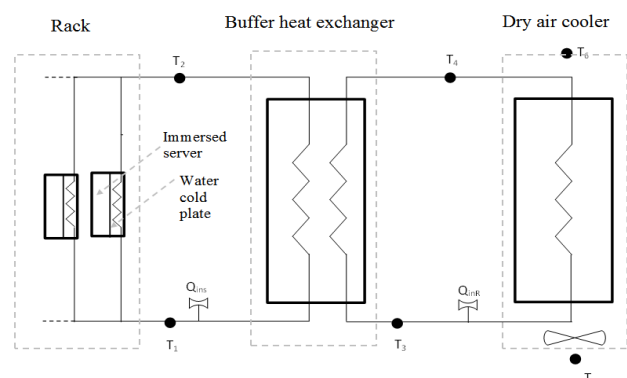


Fig.1 Schematic diagram of the data center cooling system

On the right of the figure is a dry air cooler and fan, which moves the air at the ambient outside temperature (T_5)

*Corresponding author: A. Almanea

through the heat exchanger. A pump circulates the water from the dry air cooler heat exchanger to a buffer (liquid-to-liquid) heat exchanger at a flow rate, Q_{inr} , to reject the heat from the data center. On the left side of the figure the immersed servers are housed in the rack and are connected to the buffer heat exchanger via a liquid loop inside the data center. A second pump circulates water between the buffer heat exchanger and the racks at a flow rate, Q_{ins} . The cold (supply) temperature to the buffer heat exchanger is T_3 and the inlet (supply) water temperature to the servers is, T_1 .

The model using COMSOL is applied to simulate the heat transfer at the server level only. However, the data of dry cooler and buffer heat exchanger data are taken from an experimental study (Iyengar et al. 2012). They studied a data center cooling system experimentally, which had a cooling system arrangement that included a dry cooler, buffer heat exchanger and servers that were cooled by a combination of pumped water cold plates on the CPU and air, via fans, for the rest of the server.

In this study, the server is fully immersed without any air used to cool the servers. Therefore, the relative humidity is not considered in the system. This gives an advantage of limiting the number of variables to be only the temperature. The ambient temperature, T_5 , is chosen for the city of Leeds, England (Jensen 2013). The annual average temperature of Leeds is shown in Fig. 2.

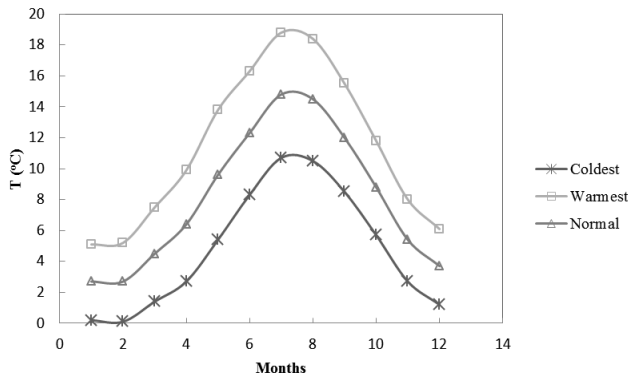


Fig. 2 Average temperature of Leeds, England (Jensen 2013)

3. Methodology of flow rate and temperature calculation

In the previous section, the data center cooling system and method of obtaining the ambient temperature, T_5 , were explained. This section develops an approach to determine the other system parameters, which are the flow rate from dry cooler to buffer heat exchange, Q_{inr} , the flow rate from the buffer heat exchanger to the rack, Q_{ins} , the cold (supply) water temperature entering the buffer heat exchanger, T_3 , and the water inlet temperature of server, T_1 .

The values of the flow rates, Q_{ins} and Q_{inr} are 5, 7.5, 10 GPM, which are taken from experimental work (Iyengar, David et al. 2012) as explained in section 2. In (Iyengar, David et al. 2012), a graph is plotted between ΔT_{apr} and the flow rate, Q_{inr} , for dry cooler fan speeds of 169 rpm.

The ΔT_{apr} is the temperature difference between the ambient temperature, T_5 , and the inlet water temperature of buffer heat exchanger, T_3 . The flow rate, Q_{ins} , and dry air cooler fan speed used are taken directly from (Iyengar, David et al. 2012), however the cooling load is different.

In (Iyengar, David et al. 2012) the ΔT_{apr} is varied with Q_{inr} has been plotted at a cooling load of 15,000 W, where the rack cooling load in this work is 5000 W (each server load is 100 W and the number of servers in one rack is 50 servers). As the flow rate and fan speed are the same as used in (Iyengar, David et al. 2012) and the heat load is different, the ΔT_{apr} is scaled down by interpolating between two rack heat load, 5000W and 15000W. Fig. 3 shows the variation of ΔT_{apr} at different flow rates, Q_{inr} , where the fan of dry cooler is spinning at 196 rpm and a cooling load of 5000 W.

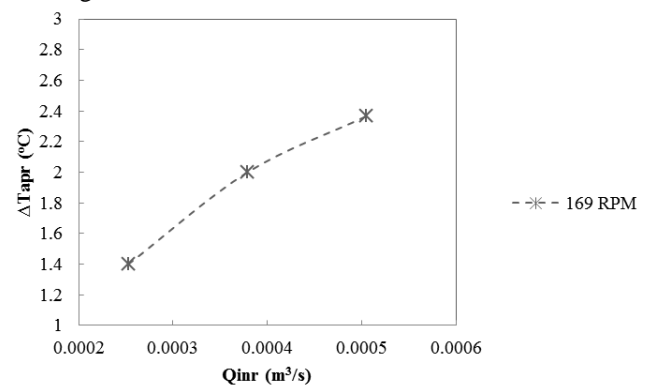


Fig 3 The variation of ΔT_{apr} with flow rate Q_{inr} , dry cooler fan spins at 169 rpm.

The flow rate, Q_{inr} , is function of ΔT_{apr} and this function is obtained from curve fitting the graph in Figure 3, it is expressed as:

$$\Delta T_{apr} = -7 \times 10^6 Q_{inr}^2 + 9366.8 Q_{inr} - 0.5$$

The flow rate between the dry cooler and the buffer heat exchanger, Q_{inr} , is known, so the ΔT_{apr} can be calculated from the equation above and the inlet water temperature to the buffer heat exchanger, T_3 , can be evaluated using

$$T_3 = T_5 + \Delta T_{apr}$$

Having obtained the value of T_3 , the next step is to determine the inlet water temperature to the servers, T_1 . The value of T_1 is based on ΔT_{aps} , which is the temperature difference between the water temperature entering the buffer heat exchanger, T_3 , and the inlet water temperature to the rack, T_1 , based on the following relationship

$$T_1 = T_3 + \Delta T_{aps}$$

The value of ΔT_{aps} is conducted from Q_{ins} and Q_{inr} . The values of Q_{ins} and Q_{inr} are varying at 5, 7.5 and 10 GPM. In (Iyengar, David et al. 2012) the graph lines for ΔT_{aps} varying with Q_{ins} and Q_{inr} which is done at cooling load 15,000 W. In this section the rack cooling load is 5000 W and the flow rate is kept the same as in the experimental

work, (Iyengar, David et al. 2012), however the cooling load is different so ΔT_{aps} is scaled down as explained before. Fig. 4 shows the variation of ΔT_{aps} for a 5000 W cooling load for different flow rates from the dry air cooler heat exchanger to buffer heat exchanger and from the rack to the buffer heat exchanger.

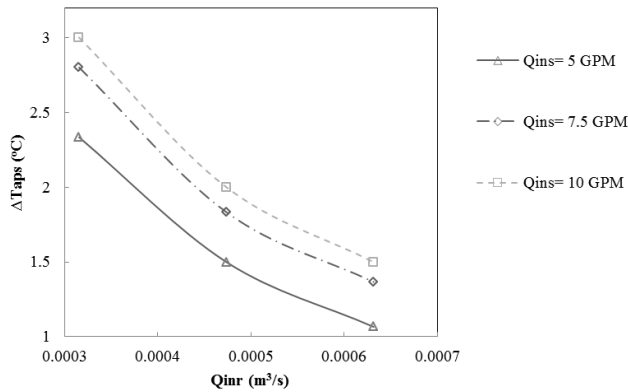


Fig 4 The variation of ΔT_{aps} with Q_{ins} and Q_{inr}

The ΔT_{aps} is affected by the Q_{ins} and the Q_{inr} variation and the relation can be obtained by fitting curves from the results in Fig.4. The equations of ΔT_{aps} can be expressed as:

At $Q_{ins} = 5$ GPM

$$\Delta T_{aps} = 8 \times 10^6 Q_{inr}^2 - 11609 Q_{inr} + 5.2$$

At $Q_{ins} = 7.5$ GPM

$$\Delta T_{aps} = 1 \times 10^7 Q_{inr}^2 - 14037 Q_{inr} + 6.23$$

At $Q_{ins} = 10$ GPM

$$\Delta T_{aps} = 1 \times 10^7 Q_{inr}^2 - 14248 Q_{inr} + 6.5$$

The M script in MATLAB v7.11 is used to solve all above equations to find the inlet water temperature of the rack, T_1 . The flow chart of the programming steps is shown in Fig. 5.

4. Results of rack inlet temperature

This section presents the results of the rack water inlet temperature, T_1 , which is obtained from MATLAB. The ambient temperature that is selected from Fig. 2 is $T_5 = 19$ °C which is the highest temperature of the year in Leeds (Jensen 2013). There are two flow rates through the buffer heat exchanger the first one is the flow rate from dry air cooler heat exchanger to buffer heat exchanger, Q_{inr} , and the second flow rate is from the buffer heat exchanger to the rack, Q_{ins} . The flow rates, Q_{ins} and Q_{inr} , are set independently to a value from 5, 7.5 and 10 GPM.

The effects of varying the flow rates on the rack water inlet temperature, T_1 , are presented in Fig. 6. Both flow rates, Q_{ins} and Q_{inr} , are varied independently between the values 5, 7.5 and 10 GPM. The results show that T_1 decreases with increasing Q_{inr} and decreasing Q_{ins} . The lowest T_1 value is found to occur, at the highest Q_{inr} and lowest Q_{ins} .

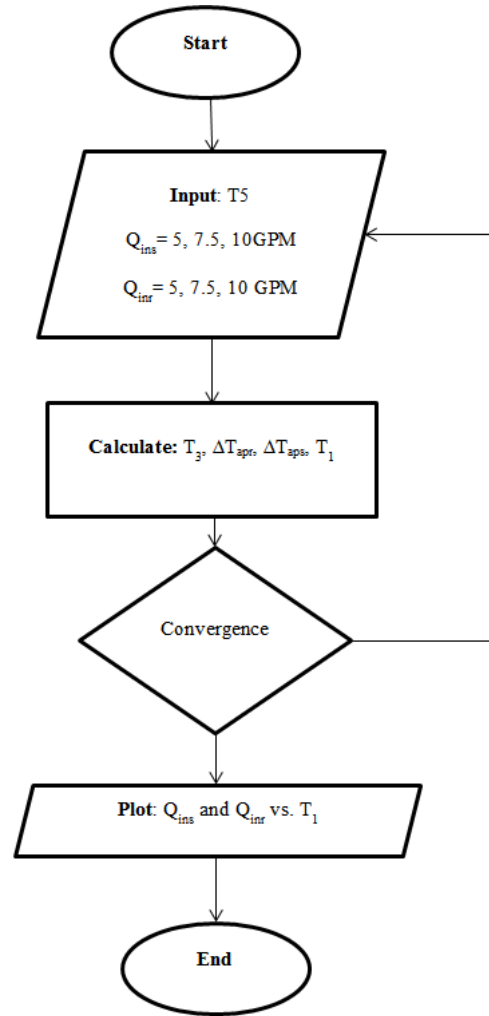


Fig 5 Flow chart of calculations to find T_1 using MATLAB v7.11

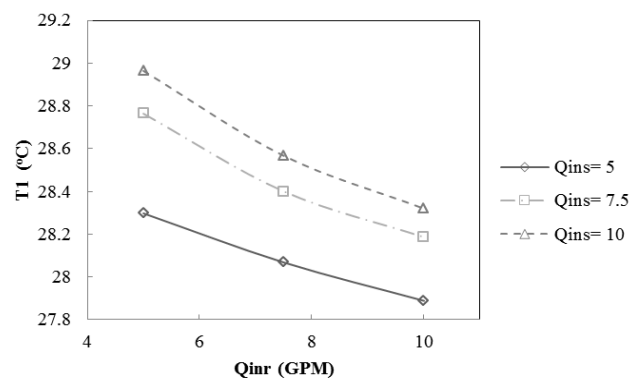


Fig 6 Water inlet temperature of rack, T_1 , varying Q_{inr} for different Q_{ins} .

From the above results the lowest water inlet temperature to the rack is found to be $T_1 = 27.9$ °C at $Q_{ins} = 5$ GPM.

5. Simulation model and results

The geometry and boundary condition of the liquid immersed server model is shown in Fig. 7. Heat is generated from the CPU underneath the heat sink and cooled by the water that passes through the cooler solid

block representing the water jacket at $T_{j=27.9}^{\circ}\text{C}$ and $Q_{ins}=5\text{ GPM}$. The conjugate heat model with symmetry planes for the immersed server is simulated via COMSOL 4.3. The simulation model set up is validated against the experimental work of natural heat convection in (Nada 2007), where a 320mm x 200mm x 40mm enclosure with fins attached on the hot wall. The buoyancy drives the flow inside the enclosure due to the temperature difference between the hot and cold walls. The average error between the simulation model presented here and the experimental work is 4.8%.

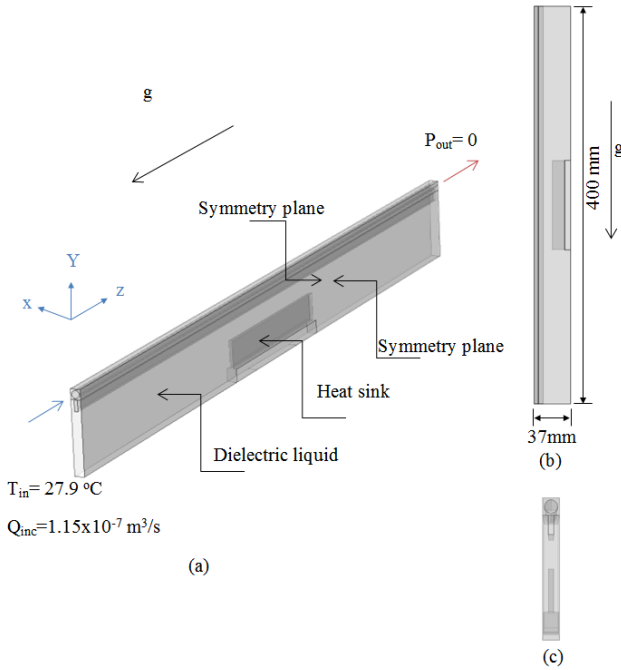


Fig 7 The geometry of the symmetry simulation model used in COMSOL a) Isometric view b) Side view c) Front View

In this study, the model consists of two types of fluid flow. The dielectric liquid is circulating inside the server due to natural convection and the other fluid is flowing by forced convection through the channel. Before solving the full conjugate heat model, the two fluid flows are checked to determine whether the flow is turbulent. For the water flowing in the channel this is determined by calculating the Reynolds number, R_e

$$R_e = \frac{\rho_w V D}{\mu_w}$$

Where D is the water channel diameter ($3.5 \times 10^{-3}\text{ m}$), V is the average flow velocity ($1.2 \times 10^{-2}\text{ m/s}$), ρ_w (996.6 kg/m^3) and μ_w ($7.96 \times 10^{-4}\text{ pa.s}$) are the density and viscosity of water, respectively. The R_e is 53 for a flow rate of $1.15 \times 10^{-7}\text{ m}^3/\text{s}$ and can therefore be considered as laminar (Çengel et al. 2008).

For natural convection inside the server, the dielectric fluid flow behaviour can be indicated by using Rayleigh number (Phan-Thien 2000), R_a

$$R_a = \frac{g\beta(T_h - T_c)H^3\rho_D^2 c_p}{\lambda_D \mu_D}$$

Where H is the server height, q is the heat flux per unit area, g is the acceleration of gravity, c_p is Specific heat capacity, ρ_D is density, λ_D is the thermal conductivity, μ_D is viscosity, β is the coefficient of volumetric expansion. All these fluid thermal properties are taken from Chi et al (Chi 2014) and listed in Table 1. The R_a is equal to 1.8×10^8 , which is greater than 10^7 and indicates therefore that the flow is turbulent (Holman 2002).

Inside the server the fluid flow is turbulent and governed by the conservation equations for mass, momentum and energy for turbulent natural convection of the dielectric liquid domain,

Continuity equation

$$\nabla \cdot (\rho \mathbf{u}_D) = 0$$

Momentum equation

$$\rho(\mathbf{u}_D \cdot \nabla) \mathbf{u}_D = \nabla \cdot \left[-p\mathbf{I} + (\mu_D + \mu_{DT})(\nabla \mathbf{u}_D + (\nabla \mathbf{u}_D)^T) - \frac{2}{3}(\mu_D + \mu_{DT})(\nabla \cdot \mathbf{u}_D)\mathbf{I} - \frac{2}{3}\rho k\mathbf{I} \right] + \mathbf{F}$$

The body force is \mathbf{F} which mainly depends on the density variation. The temperature increases the density of the fluid decreases. This driving buoyancy force which can be expressed as:

$$\mathbf{F} = \rho(T)\mathbf{g}$$

Where $\mathbf{g} = (0, 0, g)$.

The dielectric fluid has density-temperature variations

$$\rho(T) = 1716.2 - 2.2T$$

In turbulent natural convection in enclosures, the $k-\omega$ turbulent model has been found to be a robust model which can offer solutions close to experimental results as investigated in (Zitzmann et al. 2005; Aounallah et al. 2007; Rundle et al. 2007). The $k-\omega$ turbulent models introduce two additional variables turbulent kinetic energy, k , and specific dissipation rate, ω . The transport equations are based on (Wilcox 1998), which are applied in the CFD model are:

$$\rho(\mathbf{u}_D \cdot \nabla)k = \nabla \cdot [(\mu_D + \mu_{DT}\sigma^*)\nabla k] + p_k - \rho\beta^*k\omega$$

$$\rho(\mathbf{u}_D \cdot \nabla)\omega = \nabla \cdot [(\mu_D + \mu_{DT}\sigma_\omega)\nabla \omega] + \alpha \frac{\omega}{k} p_k - \rho\beta_0\omega^2$$

The turbulent viscosity can be defined as

$$\mu_{DT} = \rho \frac{k}{\omega}$$

The production term is found from the fluid velocity as

$$p_k = \mu_{DT} \left[\nabla \mathbf{u}_D : (\nabla \mathbf{u}_D + (\nabla \mathbf{u}_D)^T) - \frac{2}{3}(\nabla \cdot \mathbf{u}_D)^2 \right] - \frac{2}{3}\rho k \nabla \cdot \mathbf{u}_D$$

Energy equation

$$\rho c_p \mathbf{u}_D \nabla T = \nabla \cdot \left((\lambda_D + \frac{c_p \mu_{DT}}{Pr_T}) \nabla T \right)$$

Where λ_D is thermal conductivity and Pr_T is turbulent Prandtl Number (using Kays-Crawford)

The empirical turbulent model constants parameters are

$$\alpha = \frac{13}{25}, \sigma_k^* = \frac{1}{2}, \sigma_\omega = \frac{1}{2}, \beta_0 = \frac{9}{125}, \beta_0^* = \frac{9}{100}, k_v = 0.41, B = 5.2$$

For the water channel which is the forced convection laminar fluid domain, the governing equations are:

Continuity equation

$$\nabla(\rho \mathbf{u}_w) = 0$$

Momentum equation

$$\rho(\mathbf{u}_w \cdot \nabla) \mathbf{u}_w = \nabla \cdot \left[-p2\mathbf{I} + \mu_w(\nabla \mathbf{u}_w + (\nabla \mathbf{u}_w)^T) - \frac{2}{3} \mu_w(\nabla \cdot \mathbf{u}_w)\mathbf{I} \right]$$

Energy equation

$$\rho c_p \mathbf{u}_w \nabla T = \nabla \cdot (\lambda_w \nabla T)$$

In the solid domain, only the energy equation is required

$$0 = \nabla \cdot (\lambda_s \nabla T)$$

Where, the λ_s is the thermal conductivity for the solids which are Copper and Aluminium.

The material of the heat sink is copper and the baffles and cold plate are made of Aluminium alloy. The working fluids in this paper are water and a dielectric liquid (see Table 1 for properties). The water is used as cooling liquid that passes through the cold plate channel and the server is filled with the dielectric liquid for which the thermal properties are kept constant except for the density which is a function of temperature.

Table 1 Thermal properties of dielectric liquid

Properties	Abbrev.	Dielectric Fluid
Specific heat capacity	C_{pD}	1140 (J/kg.K)
Thermal expansion	β_D	$1.151496 \times 10^{-3} (K^{-1})$
Dynamic viscosity	μ_D	$1.124782 \times 10^{-3} (Pa.s)$
Thermal conductivity	λ_D	$6.9 \times 10^{-2} (W/m.K)$

A typical fluid flow inside the immersed server is shown in fig.8 (a). The heat transferred to the liquid as it flows through the CPU heat sink leads to a buoyancy-driven flow which results in the liquid rising on the left hand portion above the CPU and falling on the right side as it is cooled by the cold plate. The flow velocities below the CPU are generally smaller than those above it. The corresponding temperature field is shown in fig 8(b) and demonstrates that the liquid above the CPU is significantly hotter than that below it. The CFD analysis is very important in practice as it enables the maximum temperature of the CPU, T_{case} , which must be constrained to ensure its reliable operation, to be predicted. In the example below $T_{case}=60.4^\circ C$.

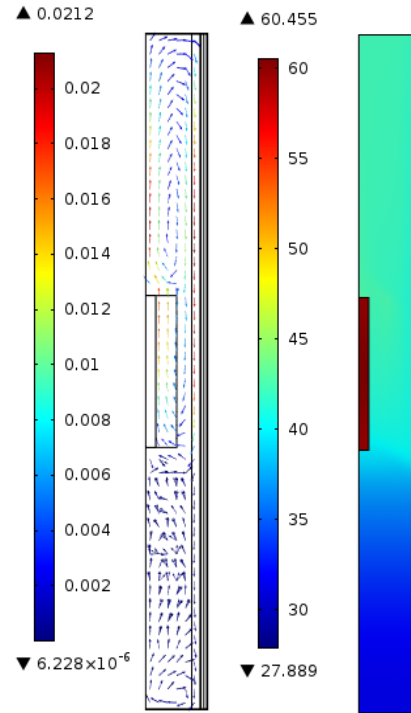


Fig 8. a) Velocity field inside the server for the dielectric liquid. b) Temperature field

The simulation model based on COMSOL 4.3b is now used to determine pressure drop in order to calculate the required pump power.

The water inlet temperature of the server channel is $T_{in} = T_1 = 27.9^\circ C$. The flow rate of the rack is $Q_{ins} = 5$ GPM and the flow rate used in the server cold plate water channel is:

Flow rate for one water channel

$$Q_{inc} = \frac{F.R.R(GPM)}{N.O.S \times N.O.C.S} = \frac{5}{50 \times 55 \times 15852} = 1.15 \times 10^{-7} \frac{m^3}{s}$$

Where F.R.R is flow rate to the rack, N.O.S is number of servers per rack and N.O.C.S is the number of water channels in one server.

The pressure drop across the water channel (ΔP_{ch}) is found be 11.6 Pa of the simulation model with temperature inlet to the server water channel equal to $27.9^\circ C$ and the water flow rate inlet server channel is $1.15 \times 10^{-7} m^3/s$.

6. PUE of cooling system

The power usage effectiveness (PUE) is used to indicate the effectiveness of the data center cooling systems and is calculated on the basis of the total power consumed by the data center relative to power that supplied the IT. A PUE of 1 means that the data center has achieved the best data center efficiency (Rouse April 2009). The equation that is used to calculate the PUE is (BELADY 2007; Haywood et al. 2012)

$$PUE = \frac{Total\ Power}{IT\ Power} = \frac{P_{IT} + P_c}{P_{IT}}$$

The power of data center utilities and power of IT is required to calculate the PUE. The power consumed by the IT in this work is coming from the rack power which is

$$P_{IT} = 50 \times 100W = 5.0 \text{ kW}$$

In this study there are two pumps to circulate water between the heat exchangers and fans to reject heat from the dry air cooler. The power of the pump, P_{ps} , that circulates the water between the rack and buffer heat exchanger is determined by (Incropera et al. 2011)

$$P_{ps} = \frac{\Delta P_s Q_{ins}}{\epsilon}$$

Where, Q_{ins} is flow rate between the rack and buffer heat exchanger, ϵ is the pump efficiency. The pressure drop from the simulation model for one channel is $\Delta P_{ch} = 11.6 \text{ Pa}$

The pressure drop for the rack is given by,

$$\Delta P_s = N.O.S \times N.O.C.S \times \Delta P_{ch} = 50 \times 55 \times 11.6 = 31.9 \text{ kPa}$$

Pump efficiencies are between 0.5 and 0.6 (Stone 2012), in this study the pump efficiency is chosen to be 0.5 for the worst case scenario. The power required pumping the water between the rack and buffer heat exchanger is

$$P_{ps} = \frac{\Delta P_s Q_{ins}}{\epsilon} = \frac{31900 \times 0.000316}{0.5} = 20.15 \text{ W}$$

The power required by the dry air cooler heat exchanger fans is based on the flow rate and pressure drop. The power of the fans calculated from,

$$P_f = \frac{\Delta P_f Q_f}{\epsilon}$$

Where the P_f is fans power, ΔP_f is pressure drop across the dry air cooler heat exchanger and Q_f is air flow rate. The ΔP_f is calculated from (Serth 2007) which is written as:

$$\Delta P_f = \frac{2f N_r Q_f^2}{\rho_a}$$

Where f is fanning friction factor, N_r number of tube rows, ρ_a is the air density and air flow rate, Q_f is calculated from $Q_f = \rho_a V_f$.

The fanning factor friction f can be determined by the flowing expression

$$f = 18.93 R_e^{-0.316} \left(\frac{P_T}{D_r} \right)^{-0.927}$$

Where R_e is Reynolds number, D_r is root diameter and P_T tube pitch. This correlation from experimental work for six rows of bank tube with parameters range:

$$2000 < R_e < 50000, 0.0186m < D_r < 0.041m, \text{ and } 0.0428m < P_T < 0.114m$$

The R_e needs to be calculated to check if this case can be applied to the experimental correlation in determining the fanning factor friction. The fans of the dry air cooler spins at rotational speeds (N) of 169 RPM and the diameter of the fans is $D_f = 0.4 \text{ m}$. Hence, the velocity is:

$$V_f = \frac{\pi D_f N}{60} = 6.19 \text{ m/s}$$

At the ambient temperature of $T_5 = 19 \text{ }^\circ\text{C}$, the thermal properties are (Çengel et al. 2008); $\rho_a = 1.2 \text{ kg/m}^3$ and $\mu_a = 18.2 \times 10^{-4} \text{ Pa.s}$

The Reynolds number can be calculated from:

$$R_e = \frac{\rho_a V_f D_r}{\mu_a} = 1.04 \times 10^4$$

Which is within the range of the experimental correlation. The D_r and P_T parameters are selected as $D_r = 0.0254 \text{ m}$ and $P_T = 0.0762 \text{ m}$ within the range of the correlation limits, thus the fanning factor fraction can be defined as:

$$f = 18.93 R_e^{-0.316} \left(\frac{P_T}{D_r} \right)^{-0.927} = 0.367$$

$$\text{And } Q_f = \rho_a V_f = 4.26 \text{ kg/m}^2.s$$

The pressure drop across the dry air cooler heat exchanger is

$$\Delta P_f = \frac{2f N_r G^2}{\rho} = 79.4 \text{ Pa}$$

The power required for one fan in the dry air cooler is,

$$P_f = \frac{\Delta P_f Q_f}{\epsilon} = \frac{794 \times 0.444}{0.7} = 72 \text{ W}$$

The dry air cooler has 5 fans and the power required for all fans yielding $P_{if} = 360 \text{ W}$.

To calculate P_c , which is the total power required for cooling $P_c = p_{ps} + p_{pr} + p_{if}$. To calculate the power of the pump that circulates the water between the dry air cooler heat exchanger and the buffer heat exchanger, p_{pr} , requires an estimate of the pressure drop. However, the pressure drop in the rack is greater than the pressure drop in the dry air cooler heat exchanger and since Q_{inr} is double Q_{ins} , assuming P_{pr} to be double to P_{ps} is a worst case scenario. The pumps, fans and IT power are all determined and hence the PUE can be calculated as:

$$PUE = \frac{\text{Total Power}}{\text{IT Power}} = \frac{P_{IT} + P_{ps} + P_{pr} + P_{if}}{P_{IT}} = \frac{5000 + 2015 + 40.3 + 360}{5000} = 1.08$$

7. PUE for different number of servers

In previous section the PUE is determined for a full rack with 50 servers. This section investigates the effect of decreasing the number of servers in a rack on the PUE. The pressure drop per server is 638 Pa. However, the flow rate passing through the rack is varying based on the number of servers. This affects the power that is required by the pumps as shown in equation.

$$P_{ps} = \frac{\Delta P_s Q_{ins}}{\epsilon}$$

Where, P_{ps} is the pumping power ΔP_s is the pressure drop across the rack, Q_{ins} is the flow rate between the rack and

buffer heat exchanger, ε is the pump efficiency. In this section, the number of servers per rack is changing from 10 to 50 servers and based on that the rack cooling load start from 1,000 to 5,000 W. The required pumping power to circulate the water between the rack and buffer heat exchanger is varying from 0.8 to 20 W. The power of circulating the water between the buffer heat exchanger and the dry air cooler heat exchanger, P_{pr} , is again assumed to be double, P_{ps} . The fan power of the dry air cooler is unchanged.

Fig. 9 shows the effect of the number of server per rack on the PUE. The results show that the PUE increases by 26% for the full rack load of 50 compared to a 20% partial rack load. Increasing the number of servers per rack decreases the PUE since the power required for the pumps, is not significantly changing with number of servers added.

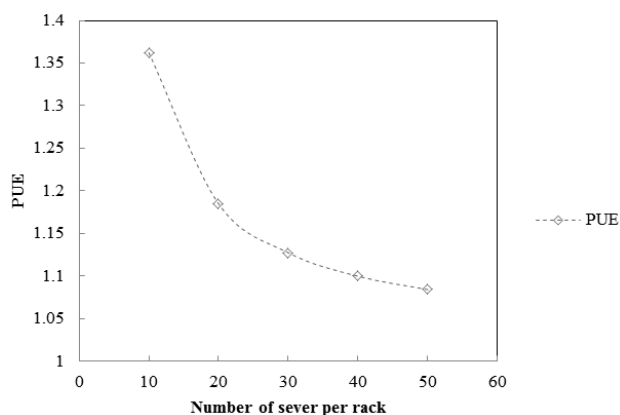


Fig 9 Variation of PUE by changing the number of the servers per rack

Conclusion

The data center cooling system in this study consists of the dry air cooler and buffer heat exchanger to dissipate the heat from a liquid cooled rack. Temperatures in the full heat rejection system are determined by combining empirical data with full CFD simulations and are based on an real geographical ambient temperature used for the dry air cooler, T_5 , of 19 °C. The data center cooling system parameters are calculated using MATLAB to obtain the inlet temperature, T_1 , and flow rate, Q_{ins} , which are used as boundary conditions for the liquid immersed server model using COMSOL to determine the pressure.

The power of the pumps is determined from the flow rate and pressures drop, which enables the PUE of data center to be calculated, yielding a data center PUE of 1.08. The effect of the PUE for different rack loads is investigated and it is found that the PUE increases by 26% for a rack-server occupancy that is 20% of maximum capacity. This is due the pump power dropping with decreasing pressure drop.

Acknowledgment

This work was inspired by the technological developments of Iceotope Research and Development based in Sheffield

(Chester, Hopton *et al.* 2013). The authors are grateful to Peter Hopton, CEO Iceotope and Yong Qiang Chi, PhD student at University of Leeds for helpful insights.

References

- R. American Society of Heating and A. C. Engineers (2006). Liquid Cooling Guidelines for Datacom Equipment Centers: ASHRAE Datacom, American Society of Heating, Refrigerating and Air-Conditioning Engineers.
- M. Aounallah, Y. Addad, *et al.* (2007). "Numerical investigation of turbulent natural convection in an inclined square cavity with a hot wavy wall." *International Journal of Heat and Mass Transfer* 50(9): 1683-1693.
- C. Belady (2007). "The green grid data centre power efficiency metrics: PUE and DCiE. White paper # 6." from http://www.thegreengrid.org/~media/WhitePapers/White_Paper_6_-_PUE_and_DCiE_Eff_Metrics_30_December_2008.pdf?lang=en.
- Y. A. Çengel, R. H. Turner, *et al.* (2008). *Fundamentals of thermal-fluid sciences* 534.
- Y. A. Çengel, R. H. Turner, *et al.* (2008). *Fundamentals of thermal-fluid sciences*, McGraw-Hill New York.
- D. Chester, P. Hopton, *et al.* (2013). *Cooled electronic system*, Google Patents.
- Y. Q. Chi, Jonathan Summers, Peter Hopton, Keith Deakin, Alan Real, Nik Kapur and Harvey Thompson (2014). *Case Study of a Data Centre Using Enclosed, Immersed, Direct Liquid-Cooled Server*. *Semiconductor Thermal Measurement and Management Symposium (SEMI-THERM)*, IEEE. 30th Annual IEEE.
- S. Greenberg, E. Mills, *et al.* (2006). "Best practices for data centers: Lessons learned from benchmarking 22 data centers." *Proceedings of the ACEEE Summer Study on Energy Efficiency in Buildings in Asilomar, CA*. ACEEE, August 3: 76-87.
- A. Haywood, J. Sherbeck, *et al.* (2012). "Thermodynamic feasibility of harvesting data center waste heat to drive an absorption chiller." *Energy Conversion and Management* 58: 26-34.
- J. Holman (2002). *Heat transfer*, 9th, McGraw-Hill: 335-337.
- P. Hopton and J. Summers (2013). *Enclosed liquid natural convection as a means of transferring heat from microelectronics to cold plates*. *Semiconductor Thermal Measurement and Management Symposium (Semi-Therm)*, 2013 29th Annual IEEE, IEEE.
- F. P. Incropera, A. S. Lavine, *et al.* (2011). *Fundamentals of heat and mass transfer*, John Wiley & Sons.
- M. Iyengar, M. David, *et al.* (2012). *Server liquid cooling with chiller-less data center design to enable significant energy savings*. *Semiconductor Thermal Measurement and Management Symposium (SEMI-THERM)*, 2012 28th Annual IEEE, IEEE.
- I. S. Jensen (2013). "Weather statistics for Leeds, England (United Kingdom)." Retrieved 19/03, 2014, from http://www.yr.no/place/United_Kingdom/England/Leeds/statistics.html
- S. Nada (2007). "Natural convection heat transfer in horizontal and vertical closed narrow enclosures with heated rectangular finned base plate." *International journal of heat and mass transfer* 50(3): 667-679.
- Y. L. Phan-Thien, Nhan (2000). "An optimum spacing problem for three chips mounted on a vertical substrate in

- an enclosure." Numerical Heat Transfer: Part A: Applications 37(6): 613-630.
- M. Rouse (April 2009). "power usage effectiveness (PUE)." Retrieved 23 March, 2014, from <http://searchdatacenter.techtarget.com/definition/power-usage-effectiveness-PUE>.
- C. Rundle and M. Lightstone (2007). Validation of turbulent natural convection in a square cavity for application of CFD modelling to heat transfer and fluid flow in atria geometries. 2nd Canadian Solar Buildings Conference, Calgary.
- R. W. Serth (2007). Process heat transfer: principles and applications, Elsevier Academic Press New York.
- A. Shah, C. Patel, *et al.* (2008). Impact of rack-level compaction on the data center cooling ensemble. Thermal and Thermomechanical Phenomena in Electronic Systems, 2008. IThERM 2008. 11th Intersociety Conference on, IEEE.
- T. L. Stone (2012). "Energy efficiency in pumping technology." 2014, from <http://www.dovercorporation.com/globalnavigation/our-markets/fluids/energy-efficiency-in-pumping-technology>.
- D. C. Wilcox (1998). Turbulence modeling for CFD, DCW industries La Canada, CA.
- T. Zitzmann, M. Cook, *et al.* (2005). Simulation of steady-state natural convection using CFD. Proc. of the 9th International IBPSA Conference Building Simulation 2005, Montréal: IBPSA.